Flip-Chip High-T_c DC SQUID Magnetometer With a Ferromagnetic Flux Antenna

Michael I. Faley, Yuri V. Maslennikov, Valery P. Koshelets, and Rafal E. Dunin-Borkowski

***Abstract*—We have combined a flip-chip high-T_c dc SQUID magnetometer with a ferromagnetic flux antenna made from 250 insulated 25-μm-thick stripes of amorphous soft magnetic Vitrovac 6025 foil inserted through the pick-up loop of the superconducting flux transformer. The ferromagnetic flux antenna provides improved magnetic coupling of the high-T_c SQUID to magnetic fields of $\sim$0.4 nT/Φ_0 to $\sim$0.18 nT/Φ_0. The orientation of the stripes was chosen to be normal to the foil tape rolling direction in order to minimize contributions from Barkhausen noise. A magnetic field resolution of $\sim$2 fT/$\sqrt{\text{Hz}}$ at 1 kHz and 77 K was achieved. Details of the technology and noise spectra of the novel composite high-T_c SQUID sensor are presented and their prospective applications for biomagnetic research and nondestructive evaluation are discussed.**

***Index Terms*—Magnetic flux, amorphous magnetic materials, high-temperature superconductors, SQUIDs, magnetic sensors.**

I. Introduction

THE high sensitivity of superconducting quantum interference devices (SQUIDs) to magnetic flux is used for the sensitive measurement of different physical properties [1]–[4]. Traditionally, SQUIDs that are intended for sensitive magnetic field measurement are equipped with multilayer superconducting flux transformers that have relatively large area pick-up coils. A superconducting flux transformer inductively concentrates magnetic flux from a larger area pick-up loop into a SQUID loop equipped with a suitable superconducting washer. Flip-chip high-T_c DC SQUID magnetometers with 20 mm multilayer superconducting flux transformers have demonstrated magnetic field resolutions of $\sim$4 fT/$\sqrt{\text{Hz}}$ at 77 K and have been used for magnetoencephalography [5], [6]. The size of a pick-up coil and its standoff distance from a room-temperature object limits the spatial resolution and information content of SQUID-based biomagnetic measurements [7]. The coupling of magnetic fields generated by μm-size objects to a SQUID can be improved by using a ferromagnetic antenna attached to the pick-up loop of a directly coupled DC SQUID [8], [9] or inserted through the pick-up loop [10]. Vitrovac 6025 has been used as material of a low noise ferromagnetic core in the pick-up coil of a low-T_c SQUID to measure currents for the investigation of two-dimensional electron gases in quantum hall effect samples at a resolution of $\sim$50 fA/$\sqrt{\text{Hz}}$ at 4.2 K with a 1 Hz bandwidth and a source resistance of $R = 12.9$ kΩ [11]. SQUIDs with Vitrovac cores in their pick-up loops have also been used to record ion beam currents in accelerometers by the non-invasive measurement of magnetic fields generated by the moving charged elementary particles (electrons or $^{20}Ne^{10+}$ ions), achieving a resolution of $\sim$6 pA/$\sqrt{\text{Hz}}$ at 4.2 K and 2 kHz [12]. By using a ferromagnetic-core-free high-T_c SQUID monitor operating at 77 K, the intensity of a 1 μA beam of $^{132}Xe^{20+}$ (50 MeV/u) ions was measured non-invasively with 100 nA resolution [13]. In the present study, we describe an implementation of a multi-stripe ferromagnetic antenna to further improve the magnetic field resolution of a flip-chip high-T_c SQUID magnetometer with a 20 mm multilayer high-T_c superconducting flux transformer that is intended for applications in biomagnetic measurements and non-destructive evaluations.

Manuscript received September 19, 2017; accepted January 4, 2018. Date of publication January 9, 2018; date of current version February 2, 2018. This work was supported in part by the European Research Council under the European Union's Seventh Framework Programme (FP7/2007-2013)/ERC under Grant 320832 and in part by the Russian Science Foundation under Grant 15-19-00206. *(Corresponding author: Michael I. Faley.)*

M. I. Faley and R. E. Dunin-Borkowski are with the Peter Grünberg Institute, Forschungszentrum Jülich GmbH, Jülich 52428, Germany (e-mail: m.faley@fz-juelich.de).

Y. V. Maslennikov and V. P. Koshelets are with the Kotel'nikov Institute of Radio Engineering & Electronics RAS, Moscow 125009, Russia (e-mail: valery@hitech.cplire.ru).

Color versions of one or more of the figures in this paper are available online at http://ieeexplore.ieee.org.

Digital Object Identifier 10.1109/TASC.2018.2791414

II. Experimental Details

A high-T_c SQUID with graphoepitaxial step-edge Josephson junctions was fabricated on a single crystalline MgO substrate, combined with a 20 mm multilayer superconducting flux transformer in a flip-chip configuration and a soft magnetic flux antenna was inserted through the pick-up loop of the flux transformer. The three major parts of the magnetometer are the high-T_c DC SQUID, the 20 mm high-T_c superconducting multilayer flux transformer and the soft magnetic flux antenna. Details of the preparation and assembly of these parts into the encapsulated magnetometer are described in the following sections.

A. High-T_c DC SQUID With Graphoepitaxial Step-Edge Josephson Junctions

A high-T_c DC SQUID with graphoepitaxial step-edge Josephson junctions, a 1 mm washer and a 4 mm directly coupled pick-up loop was prepared on a 10 mm $\times$ 10 mm $\times$ 1 mm single crystalline MgO (100) substrate, whose edges were oriented along the [100] and [010] directions [14]. A step with a height of $\sim$0.4 μm and a slope angle of $\sim$45° was prepared on the surface of the substrate using Ar ion beam milling and a mask of nLOF2020 photoresist. The surface of the stepped substrate was

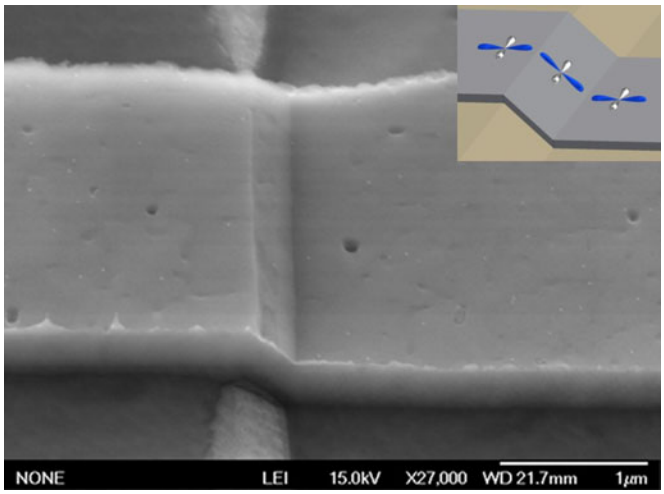

Fig. 1. SEM image of a high-T_c Josephson junction made on an ion-beam-milled 45° step edge on an MgO substrate. Inset shows a schematic representation of this junction with relative orientations of the d_{x2-y2} lobes of the order parameter in the corresponding segments of the top YBCO film.

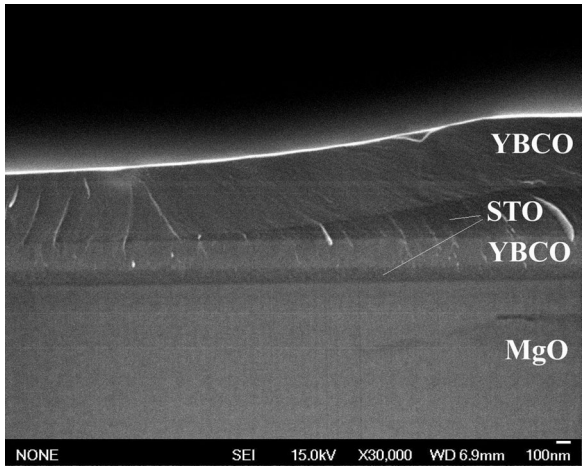

Fig. 2. Cross-sectional SEM image showing the edge area of the interconnection in the input coil of a high-T_c flux transformer prepared on a buffered MgO (100) wafer.

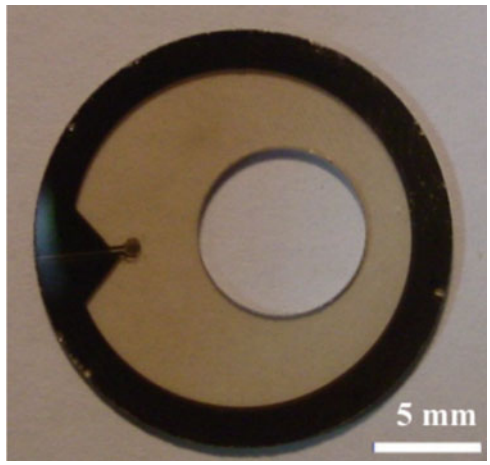

Fig. 3. Photograph of a 20 mm high-T_c superconducting multilayer flux transformer with a 14 turn input coil and a 9 mm hole in the pick-up loop.

textured using ion beam milling and buffered by a double layer consisting of a 10 nm graphoepitaxial $YBa_2Cu_3O_{7-x}$ (YBCO) seed layer and a 30-nm-thick $SrTiO_3$ (STO) "blocking" layer [6]. Finally, the top 200-nm-thick YBCO layer was deposited and structured in the form of a DC SQUID with Josephson junctions made from 2-μm-wide bridges crossing the step edges. A schematic diagram of such a Josephson junction is shown in Fig. 1. Two 45° [100]-tilted grain boundaries are formed in all of the layers, including the top YBCO film, with one boundary at the upper and the other at the lower corner of the step [6], [14], [15].

One 10 mm MgO substrate was sufficient for the production of four high quality SQUIDs, which were separated from each other by a diamond wire saw. The ends of a twisted pair of insulated Cu wires were fixed using 0.5 mm pieces of In on the opposite side of the substrate and contacted to the SQUID electrodes using Pt and Ag films.

B. High-T_c Superconducting Multilayer Flux Transformer

A superconducting flux transformer collects the flux of a magnetic field under investigation and transforms it into a larger magnetic flux through a SQUID loop with the help of a multilayer multiturn input coil that is inductively coupled to the SQUID loop. A high-T_c superconducting multilayer flux transformer with a round 20 mm pick-up loop and a 14-turn input coil was prepared on a buffered 1-mm-thick MgO (100) wafer. Fig. 2 shows a cross-sectional scanning electron microscopy (SEM) image of an edge area of the interconnection between two epitaxial YBCO layers in the input coil of the flux transformer. In order to provide a cube-on-cube in-plane orientation of the films, the surface of the wafer was textured using ion beam milling and covered by a 5-nm-thick $BaZrO_3$ film (not shown in Fig. 2). Two high-T_c superconducting layers of YBCO were separated by a 500-nm-thick insulating layer consisting of $PrBa_2Cu_3O_{7-x}$ (PBCO) and STO films. (The two PBCO films are ~10 nm thick and are not indicated in Fig. 2). The lower YBCO film was structured by chemical wet etching in a Br-ethanol solution [16]. The gently sloping edges of the patterned structures are advantageous for avoiding the formation of grain boundaries in the upper YBCO layer.

The input coil includes a ~200 nm lower YBCO film covered by a ~400 nm layer of PBCO-STO insulator and a 500-nm-thick upper YBCO film. Sufficiently long oxygenation of both YBCO layers (for ~2 hours) was performed inside the sputtering machine at a substrate temperature of ~500 °C. The insulating layer allows sufficient diffusion of oxygen ions through it into the lower YBCO film under these conditions. Both gently sloping edges of the patterned structures and full oxygenation of the YBCO films are required to achieve low 1/f noise in the high-T_c superconducting multilayer flux transformer.

A 9 mm hole for a magnetic flux antenna was drilled through the pick-up loop of the flux transformer (see Fig. 3) by mechanical milling using an Ultrasonic 20 Linear robotic machine (SAUER GmbH) with 2 mm diamond milling cutter tools.

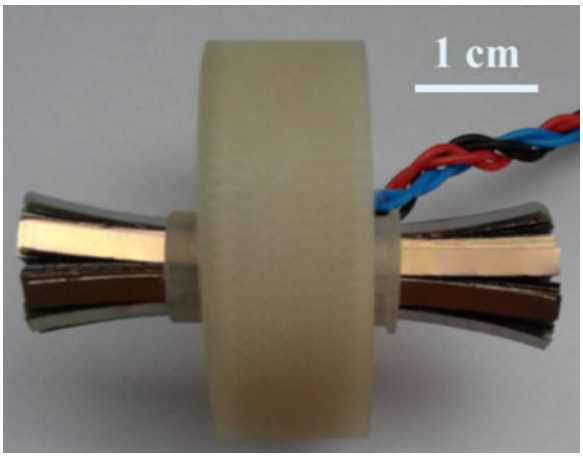

Fig. 4. Photograph of the encapsulated high-T_c DC SQUID magnetometer, with the multi-stripe soft magnetic flux antenna inserted through the pick-up loop of the flux transformer.

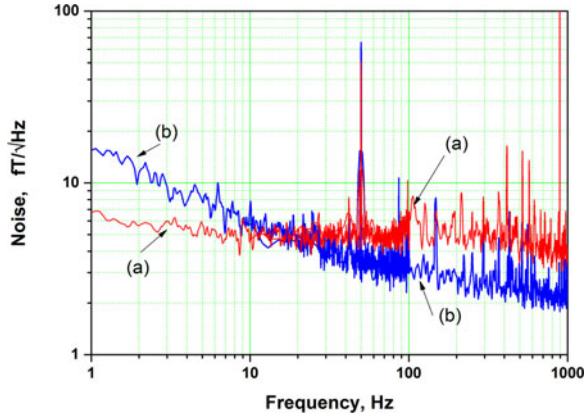

Fig. 5. Noise spectra of the high-T_c DC SQUID magnetometer measured at 77 K (a) without a ferromagnetic antenna and (b) with a ferromagnetic antenna measured inside μ-metal tubes and a double-walled cylindrical shield made from a double-sided YBCO thick-film coating on an yttria stabilized zirconia tube.

C. Soft Magnetic Flux Antenna

As in our previous experiments [10], we used an amorphous soft magnetic 25-μm-thick foil made from Fe-Mo-Co-B-Si-alloy Vitrovac 6025X (VACUUMSCHMELZE GmbH & Co. KG) for the magnetic flux antenna. In the present study, we used the same foil covered on both sides by a 200 nm insulating film of aluminum oxide (Al_2O_3), which was cut into 2-mm-wide 35-mm-long stripes by a laser and ceramic scissors. The orientation of the stripes was chosen to be normal to the tape rolling direction, in order to achieve continuous rotation of magnetic domains in the entire composite material in the presence of weak magnetic fields.

D. Assembly of the High-T_c DC SQUID Magnetometer

A Pt heater and the SQUID were fixed on the flux transformer in a flip-chip configuration using non-corrosive glue and encapsulated in a fiberglass capsule that had holes on opposite sides. A fiberglass hollow cylinder with an inner diameter $d = 6$ mm was inserted into all three holes and filled by $\sim$250 stripes of Vitrovac 6025 (see Fig. 4). In this way, the multi-stripe soft magnetic flux antenna was inserted through the pick-up loop of the flux transformer. Finally, vacuum-tight sealing of the capsule was achieved using two-component glue. The ferromagnetic antenna can be inserted through the hole in the pick-up loop of the flux transformer or removed from it without opening the capsule. The soft magnetic stripes can be glued together using varnish with a filling factor of $\sim$50%, thereby creating a bulk amorphous extremely soft magnetic composite material that has significantly lower magnetic noise than bulk μ-metal.

E. Measurements and Results

DC SQUID control electronics with a 2 kHz bias-reversal modulation and a white noise level of $\sim$0.2 nV/$\sqrt{\text{Hz}}$ referred to the input were used for operation of the magnetometer. Field-to-flux transformation coefficients $k = \partial B/\partial \Phi$B were measured using a three-layer μ-metal shield with an inner diameter of $\sim$33 cm and a residual magnetic field of $\sim$1 nT. A glass cryostat containing the SQUID was placed inside a plexiglass cylinder in the middle of a five-turn copper wire coil wound on the outer diameter ($D = 15$ cm) of the plexiglass cylinder. The magnetic field B of the coil was determined from the voltage $V(B)$ dropped on a resistance $R = 22$ kΩ connected in series with the coil, according to the expression

$$B(nT) = \frac{\mu_0 N I}{D} \approx 1.9 \cdot V(B), \tag{1}$$

where $\mu_0 = 4\pi 10^{-7}$ H/ m, $N = 5$ and $I = V/R$. For the magnetometer without a ferromagnetic antenna, the field-to-flux transformation coefficient was $\sim$0.4 nT/Φ_0. Insertion of the 4 cm ferromagnetic antenna improved this coefficient to $\sim$0.18 nT/Φ_0. Shortening of the ferromagnetic antenna to a length of 15 mm increased the field-to-flux transformation coefficient to $\sim$0.27 nT/Φ_0.

Measurements of noise spectra were performed at 77 K inside three shields made from μ-metal tubes and one high-T_c superconducting shield made from a double-sided YBCO thick film coating on an yttria stabilized zirconia tube [17] with an inner diameter of 60 mm and a length of 250 mm.

At 500 Hz, the measured values of magnetic flux noise $S^{1/2}$(500 Hz) were $\sim 10\,\mu\Phi_0/\sqrt{\text{Hz}}$, independent of the absence or presence of the ferromagnetic antenna (see Fig. 5). The knee at frequency about 600 Hz is due to low-pass filter of the SQUID readout electronics. Taking into account the corresponding field-to-flux transformation coefficients, the magnetometer with the ferromagnetic antenna demonstrated a magnetic field resolution of $\sim 2\,\text{fT}/\sqrt{\text{Hz}}$, which corresponds to an improvement by a factor of 2, when compared to a magnetic field resolution of $\sim 4\,\text{fT}/\sqrt{\text{Hz}}$ obtained using the same SQUID magnetometer without a ferromagnetic antenna. At lower frequencies, a stronger increase in noise was detected for the magnetometer with the ferromagnetic antenna. At frequencies below 10 Hz the magnetometer without the ferromagnetic antenna demonstrated a better magnetic field resolution. It was observed that the 1/f noise related to the ferromagnetic antenna was lower for better mechanical fixing of the ferromagnetic stripes relative to the pick-up loop of the flux transformer and decreased slowly with the time. These effects seem to be related to the presence

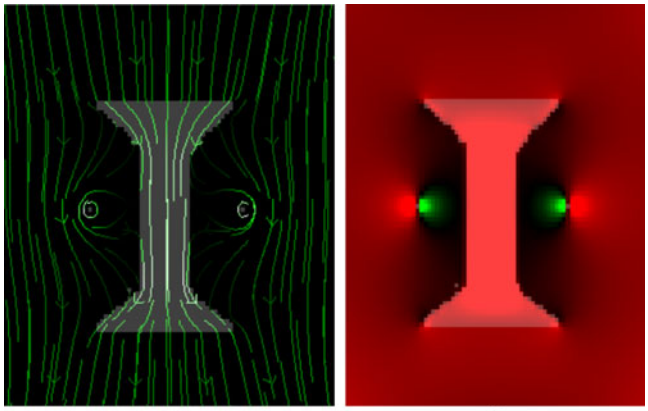

Fig. 6. Computer simulations for a current loop with a ferromagnetic antenna: (a) Magnetic field lines in the plane that includes the axis of the current loop and (b) positive (red) and negative (green) values of the component of magnetic field parallel to the axis of the current loop.

of residual mechanical vibrations in the measurement system and to relaxation of the magnetic domain structure in the stripes after movement of the ferromagnetic antenna with the SQUID into the magnetically shielded environment.

The described magnetometer demonstrated long term stability and it is robust with respect thermal cycle. No increase of the flux noise after more than ten thermal cycles was observed.

III. Discussion

A ferromagnetic antenna that penetrates the pick-up loop of a high-T_c flux transformer helps to couple magnetic flux to the SQUID loop. More magnetic field lines can then be collected by the pick-up loop, as shown in the form of computer simulations in Fig 6 where Fig. 6(a) shows magnetic field lines in the plane that includes the axis of the current loop. Fig. 6(b) shows positive (red) and negative (green) values of the component of magnetic field parallel to the axis of the current loop. For homogeneous magnetic fields generated by distant objects, this approach results in an improvement in the magnetic field resolution of a high-T_c DC SQUID magnetometer at 1 kHz by more than a factor of 2 without increasing the size of the pick-up loop. No significant increase in white noise was observed, thanks to the electrical insulation of the stripes from each other by Al_2O_3 films, which resulted in the suppression of Nyquist noise in the antenna. The stronger frequency dependence of intrinsic noise observed when using the ferromagnetic antenna can be attributed to residual Barkhausen noise in the stripes and is considerably lower than when using other ferromagnetic materials.

The dependence of the field-to-flux transformation coefficient on the lengths $L_1 = 15$ mm and $L_2 = 35$ mm of a ferromagnetic antenna of central diameter $d_1 = 6$ mm can be described by a demagnetization coefficient along the antenna, which is given by the expression [18]

$$N_z\left(m_{1,2}\right) = \frac{\ln(2m_{1,2}) - 1}{m_{1,2}^2}, \tag{2}$$

where $m_{1,2} = L_{1,2}/d_1$. The effective magnetic permeability of the flux antenna in the pick-up loop μ_{eff} can be estimated from the related expression for a "Diabolo"-shaped ferromagnetic core [19], [20]:

$$\mu_{eff} = \frac{\mu_r}{1 + N_z \frac{d_1^2}{d_2^2}\left(\mu_r - 1\right)}, \tag{3}$$

where $d_2 = 10$ mm is the diameter of the core at its ends and the magnetic permeability μ_r of Vitrovac 6025 is ~70 000.

This approach can be used to improve the sensitivity of biomagnetic measurements, for non-destructive tests, in geomagnetic surveys, for energy-efficient monitoring of beam currents in ion accelerators, etc. Such a ferromagnetic antenna can be used to provide improved sensitivity and spatial resolution by the prolongation of the magnetic antenna to the surface of investigated object and by directing the magnetic flux through the pick-up loop and back to the room temperature object, just as in a SQUID microscope [10] or in the write/read heads of magnetic computer hard discs. Depending on the configuration of the magnetic flux antenna, different components of local magnetic fields from the room temperature object can be measured.

High-T_c SQUID systems for non-destructive evaluation, geomagnetic surveys and systems intended for monitoring beam currents in ion accelerators will achieve better sensitivity at lower frequencies at an operating temperature of 77 K, as well as resulting in new possibilities for the construction of gradiometric configurations of sensors and magnetic shields. Further improvements in the magnetic field resolution of high-T_c SQUID sensors over all frequencies, while maintaining spatial resolution, are possible by optimizing the configuration of the ferromagnetic antenna and by further minimizing vibrations.

IV. Conclusion

Without using a ferromagnetic flux antenna, the flux-to-field transformation coefficient of the magnetometer described in this paper was $\sim 0.4\,\mathrm{nT}/\Phi_0$, with a magnetic flux noise of $\sim 10\,\mu\Phi_0/\sqrt{\mathrm{Hz}}$ and a magnetic field resolution of $\sim 4\,\mathrm{fT}/\sqrt{\mathrm{Hz}}$ at 77 K. The use of a novel ferromagnetic antenna was shown to improve the flux-to-field transformation coefficient to $\sim 0.18\,\mathrm{nT}/\Phi_0$ and the magnetic field resolution by approximately a factor of 2 to $\sim 2\,\mathrm{fT}/\sqrt{\mathrm{Hz}}$ at 77 K and a frequency of ~1 kHz, while leaving the magnetic flux noise nearly unchanged. At lower frequencies, a stronger increase in noise was detected for the magnetometer with the ferromagnetic antenna at frequencies below 10 Hz, with the magnetometer without a ferromagnetic antenna demonstrating better magnetic field resolution.

Acknowledgment

The authors gratefully acknowledge valuable discussions with U. Poppe and T. Watanabe and the technical assistance of R. Speen and A. Enns.

References

[1] J. Clarke and A. I. Braginski, Eds., *The SQUID Handbook vol. 2: Applications of SQUIDs and SQUID Systems*. Weinheim, Germany: Wiley, 2006.

[2] P. Seidel, Ed., *Applied Superconductivity: Handbook on Devices and Applications*, vol. 2. Weinheim, Germany: Wiley, 2015.
[3] C. Granata and A. Vettoliere "Nano superconducting quantum interference device: A powerful tool for nanoscale investigations," *Phys. Rep.*, vol. 614, pp. 1–69, 2016.
[4] D. Koelle, R. Kleiner, F. Ludwig, E. Dantsker, and J. Clarke, "High transition temperature superconducting quantum interference devices," *Rev. Mod. Phys.*, vol. 71, pp. 631–686, 1999.
[5] M. I. Faley *et al.*, "Integration issues of graphoepitaxial high-T_c SQUIDs into multichannel MEG systems," *IEEE Trans. Appl. Supercond.*, vol. 25, no. 3, Jun. 2015, Art. no. 1601605.
[6] M. I. Faley *et al.*, "High-T_c SQUID biomagnetometers," *Superconductor Sci. Technol.*, vol. 30, 2017, Art. no. 083001.
[7] J. F. Schneiderman, "Information content with low-vs. high-T_c SQUID arrays in MEG recordings: The case for high-T_c SQUID-based MEG," *J. Neurosci. Methods*, vol. 222, pp. 42–46, 2014.
[8] S. A. Gudoshnikov *et al.*, "Magnetic flux guide for high-resolution SQUID microscope," *IEEE Trans. Appl. Supercond.*, vol. 11, no. 1, pp. 219–222, Mar. 2001.
[9] S. Tanaka, K. Matsuda, O. Yamazaki, M. Natsume, H. Ota, and T. Mizoguchi, "Development of high-T_c SQUID microscope with flux guide," *Superconductor Sci. Technol.*, vol. 15, pp. 146–149, 2002.
[10] M. I. Faley *et al.*, "Nondestructive evaluation using a high-T_c SQUID microscope," *IEEE Trans. Appl. Supercond.*, vol. 27, no. 4, Jun. 2017, Art. no. 1600905.
[11] P. Gutmann and V. Kose, "Optimum dc current resolution of a ferromagnetic-core flux transformer coupled SQUID instrument," *IEEE Trans. Instrum. Meas.*, vol. IM-36, no. 2, pp. 267–270, Jun. 1987.
[12] A. Peters, W. Vodel, H. Koch, R. Neubert, H. Reeg, and C. H. Schroeder, "A cryogenic current comparator for the absolute measurement of nA beams," *Proc. AIP Conf.*, vol. 451, pp. 163–180, 1998.
[13] T. Watanabe, N. Fukunishi, M. Kase, O. Kamigaito, S. Inamori, and K. Kon, "Beam current monitor with a high-T_c current sensor and SQUID at the RIBF," *J. Supercond. Novel Magn.*, vol. 26, no. 4, pp. 1297–1300, 2013.
[14] M. I. Faley *et al.*, "High-T_c DC SQUIDs for magnetoencephalography," *IEEE Trans. Appl. Supercond.*, vol. 23, no. 3, part 1, Jun. 2013, Art. no. 1600705.
[15] M. I. Faley, "Reproducible step-edge Josephson junction," U.S. Patent 9666783 B2 (granted 30.05.2017), Patent DE102012006825 B4 (granted 26.02.2015), and Patent EP 2834860 B1 (granted 30.12.2015), PCT Pub, Oct. 10, 2013.
[16] M. I. Faley, U. Poppe, H. Soltner, C. L. Jia, M. Siegel, and K. Urban, "Josephson junctions, interconnects and crossovers on chemically etched edges of $YBa_2Cu_3O_7$," *Appl. Phys. Lett.*, vol. 63, no. 15, pp. 2138–2140, 1993.
[17] N. McN Alford, S. J. Penn, and T. W. Button, "High-temperature superconducting thick films," *Superconductor Sci. Technol.*, vol. 10, pp. 169–185, 1997.
[18] J. A. Osborn, "Demagnetizing factors of the general ellipsoids," *Phys. Rev.*, vol. 67, pp. 351–357, 1945.
[19] C. Coillot, J. Moutoussamy, P. Leroy, G. Chanteur, and A. Roux, "Improvements on the design of search coil magnetometer for space experiments," *Sensor Lett.*, vol. 5, pp. 167–170, 2007.
[20] C. Coillot *et al.*, "Magnetic noise contribution of the ferromagnetic core of induction magnetometers," *J. Sensors Sensor Syst.*, vol. 4, pp. 229–237, 2015.